



Contents lists available at ScienceDirect

## Ocean Modelling

journal homepage: [www.elsevier.com/locate/ocemod](http://www.elsevier.com/locate/ocemod)

## Parameterizing mesoscale eddies with residual and Eulerian schemes, and a comparison with eddy-permitting models

Rongrong Zhao, Geoffrey Vallis \*

Atmospheric and Oceanic Science Program, Princeton University, Princeton, NJ 08544, USA

### ARTICLE INFO

#### Article history:

Received 9 May 2007

Received in revised form 11 February 2008

Accepted 12 February 2008

Available online 5 March 2008

### ABSTRACT

In this paper we explore and test certain parameterization schemes that aim to represent the effects of unresolved mesoscale eddies on the larger-scale flow. In particular, we examine a scheme based on the residual or transformed Eulerian mean formulation of the equations, in which the eddies are parameterized by a large vertical viscosity in the momentum equations, with no skew flux parameterization appearing in the tracer (e.g., temperature or salinity) evolution equations, although terms that parameterize diffusion along isopycnal surfaces remain.

The residual scheme is compared both to a conventional parameterization that uses a skew diffusion (or equivalently advection by a skew velocity), and to eddy-permitting calculations. Although in principle almost equivalent to certain forms of skew flux schemes, the residual formulation is found to have certain practical advantages over the conventional scheme in some circumstances, and in particular near the upper boundary where conventional schemes are sensitive to the choice of tapering but the residual scheme is less so. The residual scheme also enables the horizontal viscosity – which is mainly applied to maintain model stability – to be reduced. Finally, the residual scheme is somewhat easier to implement, and the tracer transport is easier to interpret. On the other hand, the residual scheme gives, at least formally, a transformed velocity, not the Eulerian velocity and will not be appropriate in all circumstances.

© 2008 Elsevier Ltd. All rights reserved.

### 1. Introduction

Mesoscale eddies in the ocean have a scale of tens to hundreds of kilometers, and consequently their effects are not explicitly accounted for in coarse resolution ocean climate models that currently may have a grid spacing of over  $1^\circ$ . It is often thought that a resolution closer to  $1/6^\circ$ , probably higher in some regions of the ocean, is necessarily to account, even imperfectly, for their effects. Now, and relatedly, observations indicate that in the ocean interior diapycnal diffusion is appropriately small (e.g., [Ledwell et al., 1998](#), [Toole et al., 1994](#)) and that the motion is predominantly adiabatic; that is, advective effects dominate diffusive effects. However, in the top and (to a lesser degree) bottom boundary layers the flow may be diabatic, and both advective and diffusive effects are important. Thus, it is commonly thought that any parameterization of mesoscale eddies should be predominantly adiabatic in the ocean interior, transitioning in some way to a diabatic scheme in the mixed layer.

A widely used eddy parameterization scheme for current ocean models was developed by [Gent and McWilliams \(1990\)](#) and [Gent et al. \(1995\)](#) (hereafter GM). The GM scheme may be formulated

either as an eddy advection term or equivalently as eddy skew flux using an anti-symmetric diffusion tensor, as described by [Griffies \(1998\)](#). In either case it is applied in the tracer equations, that is in the evolution equations for temperature, salinity and any passive tracers that may be present. The GM scheme of itself is adiabatic, and as such is appropriate for the ocean interior. It has been a very successful parameterization, although its implementation in ocean models is not without its problems. In particular, diabatic effects in the upper mixed layer are often incorporated by reducing the slope along which the parameterized tracer flux occurs as the surface is approached. That is, in the adiabatic flow interior the flux is parallel to the contours, but as the surface is approached the flux is allowed to cross-isopycnal surfaces. Climate models are found to be rather sensitive to the precise way in which this is done. For instance, [Gough and Welch \(1994\)](#) found ocean models are sensitive to the tapering constants such as maximum allowable isopycnal slope, and in more recent simulations of [Gnanadesikan et al. \(2007\)](#) (using the GDFL MOM model), it is also shown that an increase on  $S_{\max}$  (a number for onset of slope tapering in GM) makes a distinctive differences in such as the vertical structure of temperature distribution, the ventilation of southern ocean, and mixed layer depth.

In conjunction with the advective GM scheme, mesoscale eddy parameterizations normally include, following [Redi \(1982\)](#), a diffusion of tracers (both active and passive) along neutral surfaces.

\* Corresponding author.

E-mail addresses: [rongrong.zhao@noaa.gov](mailto:rongrong.zhao@noaa.gov) (R. Zhao), [gkv@princeton.edu](mailto:gkv@princeton.edu) (G. Vallis).

Such diffusion must also be tapered near the surface in order that the flux be horizontal. If there is no salinity, and an equation of state of the form  $\rho = \rho(\theta)$ , then there is evidently no diffusion of temperature along isopycnal surfaces (this is the case in the simulations we perform), although the scheme will give a horizontal, and diabatic, diffusion of buoyancy near the surface.

An alternative to the conventional GM scheme is to recast the equations in residual form, using the transformed Eulerian mean. (See Andrews et al. (1987) or Vallis (2006) for general background, Greatbatch and Lamb (1990), Greatbatch and Li, 1990 and Greatbatch (1998) for theoretical analysis and discussion in an ocean context, Wardle and Marshall (2000) and Ferreira and Marshall (2006) for applications in an ocean model, and Holloway (1997) for a discussion of the relation of thickness diffusion to eddy momentum effects.) In the residual scheme, the eddy buoyancy terms are transformed away from the buoyancy equation, and reappear in the momentum equation where they combine with the eddy momentum fluxes to give potential vorticity fluxes, potentially with ensuing conceptual and computational simplifications. No eddy advection terms are needed in the tracer equations, although a Redi diffusion for each tracer must still be calculated. Also, the residual formulation does, at least formally, predict the residual velocities and not the local Eulerian velocities, which may be disadvantageous in some circumstances. Although on the one hand such a recasting may be regarded merely a formal transformation of the equations, the practical differences in implementing a parameterization scheme may be significant. Further, given the general uncertainty of any parameterization scheme, having a mesoscale parameterization in the momentum equation is at least as a priori justifiable as having one in the thermodynamic equation.

## 2. Eddy parameterizations

### 2.1. Tracer equation

The governing equation for a tracer,  $b$ , may be written

$$\frac{\partial \bar{b}}{\partial t} + \bar{\mathbf{v}} \cdot \nabla \bar{b} + \nabla \cdot \overline{\mathbf{v}'b'} = \mathbf{S} + \mathbf{D} \quad (2.1)$$

We will regard  $b$  as buoyancy, and for simplicity salinity will be absent from our considerations, a restriction that is fairly easily relaxed. In (2.1) we have decomposed the velocity in the standard way into two parts: a resolved Eulerian mean velocity  $\bar{\mathbf{v}}$ , and an unresolved perturbation  $\mathbf{v}'$ , or sub-grid scale (SGS) velocity. The overbar may be regarded as a kind of low-pass filter, acting over a coarse-grid cell that is fixed in space, with the primed variables representing motions that are unresolved on the coarse-grid. The SGS motions affect the large-scale motion through the term  $\nabla \cdot \overline{\mathbf{v}'b'}$ , and need to be parameterized in the coarse-grid model. (It may be argued that model variables should be naturally interpreted as thickness-weighted isopycnal averages, and thickness-weighting naturally leads to a residual form of the equations, but we do not pursue this line of argument here.) On the right-hand side of (2.1),  $\mathbf{S}$  is any external heating and cooling process, which are important mainly near the ocean surface. The term  $\mathbf{D}$  represents vertical and horizontal diffusive processes on the fine-scale and molecular processes, but not on the mesoscale we seek to parameterize; that is, we assume that it is meaningful to separate the parameterizations for the mesoscale and the fine scale. The term includes a vertical diffusion term,  $\partial_z(\kappa_v \partial_z b)$ , that represents the real physical process of internal wave breaking leading to a diapycnal diffusion;  $\kappa_v$  has a measurable, albeit small value, meaning that over most of the ocean interior the vertical diffusion does not enter the leading order balance of (2.1). Any horizontal

diffusion that is included in  $\mathbf{D}$ ,  $\kappa_h \nabla_h^2 b$  for example, would be less physical, being included in ocean models mainly for numerical reasons with the value for  $\kappa_h$  being dependent on the model resolution.

Let us decompose the eddy flux,  $\mathbf{F} = \overline{\mathbf{v}'b'}$ , into two parts: one that is diapycnal (i.e., across contours of  $\bar{b}$ ) and denoted  $\mathbf{F}_\perp$ , and one that is isopycnal (i.e., aligned along contours of  $\bar{b}$ ) and denoted  $\mathbf{F}_\parallel$ :

$$\overline{\mathbf{v}'b'} = \mathbf{F}_\perp + \mathbf{F}_\parallel = \frac{\overline{\mathbf{v}'b'} \cdot \nabla \bar{b}}{|\nabla \bar{b}|^2} \nabla \bar{b} - \frac{\overline{\mathbf{v}'b'} \times \nabla \bar{b}}{|\nabla \bar{b}|^2} \times \nabla \bar{b} \quad (2.2)$$

This is a vector identity, as may be verified by expanding the vector triple product in the last term on the right-hand side. (The gradient operator in this expression is three-dimensional; the horizontal operator will be denoted  $\nabla_h$ .) The diapycnal component of eddy buoyancy flux  $\mathbf{F}_\perp$  is important primarily in the mixed layer. The along isopycnal flux  $\mathbf{F}_\parallel$ , important in both ocean interior and ocean boundary, is the main topic of current work. Eden et al. (2007) discuss such eddy flux decompositions in more detail.) Taking the divergence of the along isopycnal term in (2.2) and applying a vector identity gives

$$\nabla \cdot \mathbf{F}_\parallel = -\nabla \cdot \left\{ \frac{\overline{\mathbf{v}'b'} \times \nabla \bar{b}}{|\nabla \bar{b}|^2} \times \nabla \bar{b} \right\} = -\left\{ \nabla \times \frac{\overline{\mathbf{v}'b'} \times \nabla \bar{b}}{|\nabla \bar{b}|^2} \right\} \cdot \nabla \bar{b} \quad (2.3)$$

If we define an eddy streamfunction and eddy velocity as

$$\Psi = -\frac{\overline{\mathbf{v}'b'} \times \nabla \bar{b}}{|\nabla \bar{b}|^2}, \quad \mathbf{v}^* = \nabla \times \Psi, \quad (2.4a, b)$$

then we may write (2.1) as

$$\frac{\partial \bar{b}}{\partial t} + \bar{\mathbf{v}} \cdot \nabla \bar{b} + \mathbf{v}^* \cdot \nabla \bar{b} = \nabla \cdot \mathbf{F}_\perp + \mathbf{S} + \mathbf{D}. \quad (2.5)$$

The effect of  $\mathbf{F}_\parallel$  is evidently equivalent to an advection process by the eddy velocity  $\mathbf{v}^*$ , and so is manifestly adiabatic in that it does not change the census of  $\bar{b}$ . If  $|b_z| \gg |\nabla_h \bar{b}|$ , as is generally the case away from boundaries, then the eddy streamfunction is given by (see Appendix A for more detail)

$$\Psi \approx -\mathbf{i} \frac{\overline{v'b'}}{b_z} + \mathbf{j} \frac{\overline{ub'}}{b_z} \quad (2.6)$$

and this is the form we shall mostly be concerned with.

The diapycnal flux divergence term  $\nabla \cdot \mathbf{F}_\perp$  is often considered to be negligible in ocean interior and only important near ocean boundaries, and eddy parameterizations for tracers are often modelled using an advective scheme (using the eddy velocity  $\mathbf{v}^*$ ) for the interior ocean domain and a diffusive scheme for ocean boundary layers.

### 2.2. The residual momentum equation

If a residual velocity  $\bar{\mathbf{v}}$  is defined as the sum of  $\bar{\mathbf{v}}$  and  $\mathbf{v}^*$ , that is  $\bar{\mathbf{v}} = \bar{\mathbf{v}} + \mathbf{v}^*$  (2.5) can be written as:

$$\frac{\partial \bar{b}}{\partial t} + \bar{\mathbf{v}} \cdot \nabla \bar{b} = \nabla \cdot \mathbf{F}_\perp + \mathbf{S} + \mathbf{D} \quad (2.7)$$

If we are to use (2.7) to simulate tracers then we need an equation for the residual velocity, and we will derive this in an informal way. In a geostrophic flow, the main balance for horizontal momentum is between Coriolis force and horizontal pressure gradient:

$$\mathbf{f} \times \bar{\mathbf{u}} \approx -\nabla \phi \quad (2.8)$$

where  $\mathbf{f} = \mathbf{fk}$ . We write this in residual form by adding an eddy velocity term (A3) into both sides of the equation, giving

$$\mathbf{f} \times \tilde{\mathbf{u}} \approx -\nabla\phi + \mathbf{f} \times \mathbf{u}^* \quad (2.9)$$

$$\approx -\nabla\phi + \mathbf{f} \times \begin{pmatrix} -\partial_z(\overline{u'b'})/\partial_z\bar{b} \\ -\partial_z(\overline{v'b'})/\partial_z\bar{b} \end{pmatrix} \quad (2.10)$$

$$= -\nabla\phi + \mathbf{f} \frac{\partial}{\partial z} \begin{pmatrix} (\overline{v'b'})/\partial_z\bar{b} \\ -(\overline{u'b'})/\partial_z\bar{b} \end{pmatrix} \quad (2.11)$$

To parameterize  $\overline{u'b'}$  and  $\overline{v'b'}$  in the ocean interior we use down gradient eddy fluxes

$$\overline{u'b'} = -\kappa\bar{b}_x, \quad \overline{v'b'} = -\kappa\bar{b}_y. \quad (2.12)$$

Using this and the thermal wind relation,

$$\bar{b}_x \approx f\bar{v}_z, \quad \bar{b}_y \approx -f\bar{u}_z, \quad (2.13a, b)$$

Eq. (2.11) becomes

$$\mathbf{f} \times \tilde{\mathbf{u}} \approx -\nabla\phi + \frac{\partial}{\partial z} \left( \kappa f^2 \frac{\partial \tilde{\mathbf{u}}}{\partial z} \right). \quad (2.14)$$

If we define eddy viscosity  $\nu_e$  as

$$\nu_e \equiv \kappa \frac{f^2}{N^2} = \kappa \frac{f^2}{-(g/\rho_0)\partial^2 z/\partial^2}, \quad (2.15)$$

then, restoring advection (2.14) becomes

$$\frac{D\tilde{\mathbf{u}}}{Dt} + \mathbf{f} \times \tilde{\mathbf{u}} = -\nabla\phi + \frac{\partial \tau_m}{\partial z} + \frac{\partial}{\partial z} \left( \nu_e \frac{\partial \tilde{\mathbf{u}}}{\partial z} \right). \quad (2.16)$$

where  $\tau_m$  is the mechanical stress from the wind and viscosity, as would also appear in the non-transformed equations. A similar form was previously obtained by Greatbatch and Lamb (1990). To get the momentum equation for residual velocity, an approximation is made on (2.16) to replace  $\tilde{\mathbf{u}}$  with the residual velocity  $\mathbf{u}^*$  in the advection term and friction term. This is a good approximation at low Rossby number:  $\mathbf{u}^*$  is small comparing to  $\tilde{\mathbf{u}}$  at least in the ocean interior; the approximation is on advection and friction terms, so the dominant geostrophic balance is not affected; and the uncertainty in the parameterization itself certainly warrants an implementation of an approximated equation of residual velocity. Thus the residual form momentum equation for our simulations is

$$\frac{D\tilde{\mathbf{u}}}{Dt} + \mathbf{f} \times \tilde{\mathbf{u}} = -\nabla\phi + \frac{\partial \tau_m}{\partial z} + \frac{\partial \tau_e}{\partial z} \quad (2.17a)$$

where the eddy stress  $\tau_e$  is given by

$$\tau_e = \nu_e \frac{\partial \tilde{\mathbf{u}}}{\partial z}. \quad (2.17b)$$

except near the ocean surface as discussed in the next section. The eddy velocity of the residual scheme,  $\mathbf{u}_{rs}^*$ , satisfies

$$\mathbf{f} \times \mathbf{u}_{rs}^* = \frac{\partial}{\partial z} \left( \nu_e \frac{\partial \tilde{\mathbf{u}}}{\partial z} \right). \quad (2.18)$$

A similar evolution equation was used by Ferreira and Marshall (2006). The parameterization embodied by (2.17) is manifestly adiabatic, for it affects only the momentum equation. The parameterization goes to zero at the equator, where  $f = 0$ , if  $\kappa$  remains finite. However, our derivation is valid only for small Rossby numbers and should not be expected to work at very low latitudes. The nature of the eddy field is also different at the equator. For both of these reasons, then, the parameterization should be regarded as applying to mid-latitude eddies only.

### 2.3. The diabatic surface layer

As the top ocean boundary is approached, eddy fluxes become aligned more horizontally, whereas isopycnals become steeper due to the active vertical mixing in the mixed layer. As a consequence eddy motions are cross-isopycnal and diabatic. Therefore,

the above arguments for an adiabatic, advective parameterization are no longer suitable in this region [as noted by, among others, Treguier et al. (1997); additional discussion is to be found in Eden et al. (2007)]. A truly satisfactory theoretical framework for the behavior of eddy fluxes as the surface is approached remains to be developed, and current schemes have been designed to satisfy simple physical restrictions, such as forcing the eddy velocity to be along-surface in the surface layer. In addition, an upper bound on the magnitude on the diffusivity must be set: in the ocean interior the isopycnal slope is small and it may sensibly be used to determine the magnitude of an eddy diffusivity. However, in the mixed layer isopycnal slopes are large – potentially infinite – and the eddy diffusivity of the conventional GM scheme, and the eddy viscosity of (2.15), must be capped in order to maintain model stability.

Accordingly, eddy parameterizations may have two aspects: (i) as needed, numerical limits on parameters are set to prevent the model from going unstable; and (ii) the eddy velocity is prescribed to be horizontal, with no eddy flux across the ocean surface. Often, treatments will force the eddy velocity to be constant throughout surface diabatic layer of some specified thickness. One example is the slope tapering for GM scheme which has been implemented in present GFDL/MOM Griffies (1998), where the eddy stream function is linearly tapered off to produce a constant eddy velocity across the surface diabatic layer. This additional treatment is in part supported by some earlier analysis based on eddy-resolving simulation of Kuo et al. (2005) which shows the horizontal component of mesoscale eddy fluxes are nearly constant throughout the surface diabatic layer.

The boundary condition on the mechanical stress at the top of the ocean is obtained by setting the momentum flux equal to the wind stress at the top of the ocean; that is

$$\tau_m(z=0) = \tau_w, \quad (2.19)$$

where  $\tau_w$  is the given wind stress. The simplest treatment of the upper boundary condition on the eddy stress in the residual framework is simply to set the eddy stress equal to zero at the top, with no explicit tapering, so that  $\nu_e \partial_z \tilde{\mathbf{u}} = 0$  at  $z = 0$ . The wind stress is added as a separate term at the upper boundary. (However, this is not wholly satisfactory from a physical standpoint because one might wish to include the wind stress at the upper boundary by way of a boundary condition of the form  $\nu \partial_z \tilde{\mathbf{u}} = \tau_m$ , where  $\nu$  is a constant, but this is not possible if it is deemed that the eddy stress should be zero at the top. But if we were to choose  $\nu \partial_z \tilde{\mathbf{u}} = \tau_m$ , then the eddy stress would not necessarily integrate to zero over the domain, as required for momentum conservation.) A similar condition is applied at the bottom of the ocean, and with the mechanical stress  $\tau_m$  there being given by a linear drag, chosen to be rather larger than the standard value to partially compensate for choice of a flat bottom. In the upper ocean we have also used somewhat more elaborate two-step scheme, as follows. The first step is to cap  $\nu_e$  [defined in (2.15)] by a constant  $\nu_{\max}$  for very weakly stratified regions where  $N^2$  is small and  $\nu_e$  is large. Thus, we set

$$\nu_e^{rs} = \min(\nu_e, \nu_{\max}). \quad (2.20)$$

Now  $\nu_e^{rs}$  is the eddy viscosity that the model actually uses. Given  $\nu_e^{rs}$ , an intermediate eddy velocity  $\mathbf{u}_{\text{inter}}^*$  may be calculated that satisfies

$$\mathbf{f} \times \mathbf{u}_{\text{inter}}^* = \frac{\partial}{\partial z} \left( \nu_e^{rs} \frac{\partial \tilde{\mathbf{u}}}{\partial z} \right), \quad (2.21)$$

along with the boundary condition (2.19). No additional treatment is needed to force the eddy fluxes to be along-surface at  $z = 0$ .

The second step of the treatment is to force the eddy velocity to be constant in the top layer of specified thickness  $D_s$ , by setting  $\tau_e$  to be a linear function of  $z$ , chosen such that the eddy stress goes to

zero at the ocean top (so that the total stress is given by the wind). [Similar requirements are made by Ferreira and Marshall (2006) and Ferrari and McWilliams (pers. comm).] In our simulations we set  $D_s$  to be constant, but other potentially more physical choices are of course possible (for example, choosing the depth to be equal to a deformation radius multiplied by the isopycnal slope). Thus, the final eddy stress is given by

$$\tau_e(z) = \begin{cases} v_e^{rs} \partial \tilde{\mathbf{u}} / \partial z & \text{for } z \leq -D_s \\ \gamma v_e^{rs} \partial \tilde{\mathbf{u}} / \partial z|_{-D_s} & \text{for } z \geq -D_s \end{cases} \quad (2.22)$$

where  $\gamma$ , a tapering coefficient, goes from zero at the surface to unity at  $z = -D_s$ . The eddy velocity (if needed) then follows from  $\mathbf{f} \times \mathbf{u}_{rs}^* = \partial \tau_e / \partial z$ , and in the upper ocean the eddy velocity has, by construction, no shear. A schematic of this treatment is given in the left panel of Fig. 1, although the eddy velocity is not guaranteed to be continuous at  $z = -D_s$ . The two-step tapering generally results in a three-layer eddy velocity: an interior region ( $z < -D_s$  and  $v_e < v_{\max}$ ); an intermediate region ( $z < -D_s$  and  $v_e \geq v_{\max}$ ); and a surface region ( $z > -D_s$ ). We may note that if the vertical eddy viscosity is large, as it will be from (2.15) if the stratification is weak, then the residual velocity will in any case be nearly constant with height, so that forcing it to be constant may have little additional effect. At the ocean bottom a similar scheme may be employed. However, eddy effects are weak there and we do not taper the eddy stresses.

It is informative to compare this scheme to the slope tapering used for GM parameterization in current GFDL ocean model. In the latter scheme, the local isopycnal slope  $\mathbf{S}$  is used to calculate eddy streamfunction. As the top of ocean is approached, isopycnals become steep and  $\mathbf{S}$  needs to be capped by a constant  $S_{\max}$  to prevent the eddy streamfunction going to infinity. And in the regions where  $\mathbf{S}$  is capped, the eddy flux is forced to be constant

$$\Psi_{gm}^x(z) = \begin{cases} \kappa_{gm} S^y & \text{for } z \leq -H \\ \kappa_{gm} S_{\max} z / H & \text{for } z \geq -H \end{cases} \quad (2.23)$$

Here  $\Psi_{gm}^x$  is the zonal component of GM eddy streamfunction, and its vertical derivative results in meridional eddy velocity.  $S^y$  is the isopycnal slope in  $y-z$  plane, and  $H$  is the depth where  $S^y$  just turned to be greater than  $S_{\max}$ . As a result, the GM eddy velocity is

$$v_{gm}^* = \begin{cases} \partial(\kappa_{gm} S^y) / \partial z & \text{for } z \leq -H \\ \kappa_{gm} S_{\max} / H & \text{for } z \geq -H \end{cases} \quad (2.24)$$

This treatment thus establishes a layer of depth  $H$  for eddy velocity  $v_{gm}^*$  to be constant. The right panel of Fig. 1 plots a typical eddy velocity resulted from this slope tapering: it often produces a very sharp shear in  $v_{gm}^*$  between ocean interior and surface diabatic layer. This sharp shear is somewhat unphysical and could over effectively flatten local isopycnals, therefore falsely alter the local

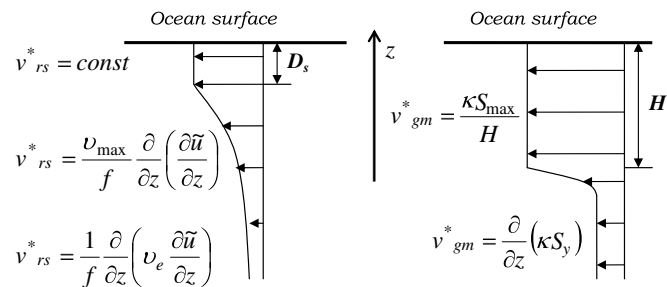


**Fig. 1.** Vertical profile of eddy velocity resulted from tapering treatments. The two-step tapering (left) of residual scheme results in a much smoother transition for eddy velocity from ocean interior to upper boundary, as comparing to slope tapering (right) of GM scheme in current GFDL climate model.

stratification. As noted in the introduction, previous studies also found that model results are sensitive to the variation of tapering parameter  $S_{\max}$ , which is mostly chosen for numerical reasons and in a somewhat arbitrary way. In our simulations, we found that the residual scheme tapering, composed of two-step treatment of (2.20) and (2.22), produces a somewhat smoother transition toward top boundary, and numerical stability is also improved. More results about this will be presented in Section 4.4.

Finally, in some simulations the horizontal mixing of buoyancy is increased in the mixed layer, via the addition of a term  $\nabla_h \cdot (\kappa_{ml} \nabla_h T)$ , with  $\kappa_{ml}$  an enhanced diffusivity. This term represents the enhanced diabatic mixing that is expected to occur in the oceanic mixed layer.

### 3. The model

We have tested the parameterization schemes described above in a primitive equation model in an idealized channel plus basin domain, as illustrated schematically in Fig. 2. The whole domain is in southern hemisphere extending from 20°S to 50°S, where the channel region is 24° in zonal extent, and 10° meridional; the gyre region is 20° zonal and 20° meridional. The domain is 3000 m deep with flat bottom. The model is both wind and buoyancy-driven; the wind distribution is also given in Fig. 2. Thermodynamic forcing is via a sea surface restoring temperature that is decreasing linearly toward the south, with 4 °C at the southern end and 18 °C at the northern end; for simplicity there is no salt.

All simulations in present work are run with GFDL/MOM4, which is  $z$ -coordinate model with hydrostatic and Boussinesq approximations. The model equations of motion are

$$\frac{\partial \mathbf{u}}{\partial t} + (\mathbf{v} \cdot \nabla) \mathbf{u} + \mathbf{f} \times \mathbf{u} = -\frac{1}{\rho_0} \nabla_h p + \frac{\partial \tau_m'}{\partial z} + \nabla_h \cdot (v_h \nabla_h \mathbf{u}) \quad (3.1)$$

$$P(z) = P_a + g \int_z^{\eta} dz' \rho \quad (3.2)$$

$$\eta_t = \nabla \cdot \mathbf{U} \quad (3.3)$$

$$\rho = \rho_0 - \alpha(T - T_0) \quad (3.4)$$

$$\frac{\partial T}{\partial t} + (\mathbf{v} \cdot \nabla) T = \frac{\partial}{\partial z} \left( \kappa_z \frac{\partial T}{\partial z} \right) + \nabla \cdot (\kappa_{GM} \nabla T) + S^T \quad (3.5)$$

Here,  $\mathbf{u}$  is the two-dimensional horizontal velocity,  $\mathbf{v}$  is the three-dimensional velocity,  $\mathbf{U}$  is the vertically integrated horizontal velocity (the 'barotropic' velocity),  $p$  is pressure,  $\eta$  is surface height,  $\rho$  is density, and  $T$  is potential temperature. The stress in (3.1) is given by  $\tau = v_z \partial_z \mathbf{u}$ ; the boundary conditions are that at the top of the model the stress is proportional the surface wind (taken as purely

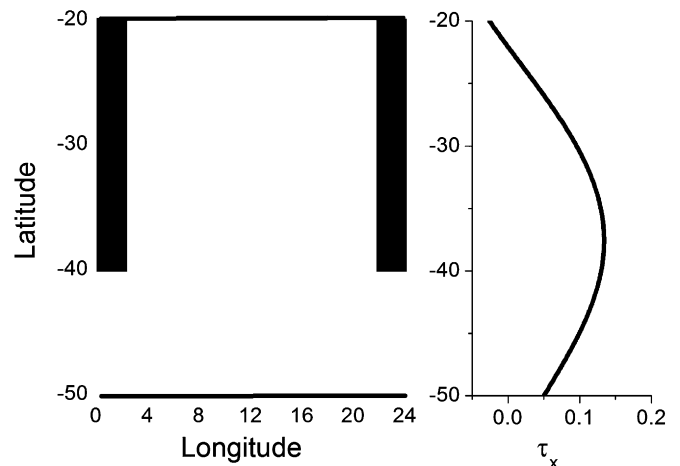


**Fig. 2.** Idealized channel model and wind stress distribution.

zonal) and at the bottom the stress is given by a linear drag. The parameter  $\kappa_z$  in (3.5) is vertical scalar diffusivity; its value, together with  $\nu_z$  and  $\nu_h$  (vertical and horizontal viscosity) are given in Table 1. (Horizontal tracer diffusivity is set to zero in all integrations, including those at coarse resolution with no GM or residual scheme.)  $S^T$  is tracer source, specifically the surface restoring heat flux.

In experiments with a conventional GM parameterization,  $\kappa_{GM}$  (the GM eddy diffusivity tensor) is non-zero and defined as

$$\kappa_{GM} = \begin{pmatrix} A_I & 0 & (A_I - A_{gm})S^x \\ 0 & A_I & (A_I - A_{gm})S^y \\ (A_I + A_{gm})S^x & (A_I + A_{gm})S^y & S^2 A_I \end{pmatrix}, \quad (3.6)$$

as in Griffies et al. (1998). It is a sum of a symmetrical tensor which accounts for isopycnal diffusion and an anti-symmetrical tensor which accounts for GM skew diffusion.  $A_I$  and  $A_{gm}$  are isopycnal diffusivity and GM skew diffusivity respectively, and we take  $A_I = A_{gm}$ . The isopycnal or Redi diffusion (Redi, 1982) has no effect in our model because of the absence of salinity, except in that as the surface is approached the combined Redi and GM fluxes are tapered to give a horizontal diffusion, similar to the explicit mixed layer diffusion term  $\nabla_h \cdot (\kappa_{ml} \nabla_h T)$  in (3.8) below. See Griffies et al. (1998) for more details as to implementation.

For experiments using the residual scheme,  $\kappa_{GM}$  is set to zero and the model was revised to accommodate the residual form momentum and tracer equations:

$$\frac{\partial \tilde{\mathbf{u}}}{\partial t} + (\tilde{\mathbf{v}} \cdot \nabla) \tilde{\mathbf{u}} + \mathbf{f} \times \tilde{\mathbf{u}} = -\frac{1}{\rho_0} \nabla_h p + \frac{\partial \tau_m}{\partial z} + \nabla_h \cdot (\nu_h \nabla_h \tilde{\mathbf{u}}) + \frac{\partial}{\partial z} \left( \nu_e^{rs} \frac{\partial \tilde{\mathbf{u}}}{\partial z} \right) \quad (3.7)$$

$$\frac{\partial T}{\partial t} + (\tilde{\mathbf{v}} \cdot \nabla) T = \frac{\partial}{\partial z} \left( \kappa_z \frac{\partial T}{\partial z} \right) + \nabla_h \cdot (\kappa_{ml} \nabla_h T) + S^T \quad (3.8)$$

Eq. (3.7) is the model version of (2.17a), with the addition of a horizontal viscosity. No slip conditions are used at the channel walls. The last term in (3.7), namely  $\partial_z (\nu_e^{rs} \tilde{\mathbf{u}}_z)$ , is the additional term introduced by the putting the eddy parameterization into residual form, and the terms  $\partial_z (\nu_z \tilde{\mathbf{u}}_z)$  and  $\nabla_h \cdot (\nu_h \nabla_h \tilde{\mathbf{u}})$  are the regular horizontal viscous terms that would appear in an Eulerian model. To account for the diapycnal diffusion which is not negligible in mixed layer (3.8) contains the diffusive term  $\nabla_h \cdot (\kappa_{ml} \nabla_h T)$ . For simplicity,  $\kappa_{ml}$  is non-zero only in the top 100 m, recognizing that a better treatment of the depth of the mixed layer will ultimately be warranted. There is no other mixed layer scheme (such as the  $k$ -profile or KPP scheme) except for a convective adjustment scheme.

We have integrated the model in essentially five different configurations: a fine-grid eddy-permitting simulation (denoted EDDY), a coarse-grid simulation with no explicit eddy parameter-

izations (denoted COARSE), a coarse-grid simulation with GM parameterization (denoted GMP), a coarse-grid simulation using residual scheme with constant eddy viscosity  $\nu_e$  (denoted RS\_NU), and a coarse-grid simulation using residual scheme with constant eddy diffusivity  $\kappa$  (denoted RS\_KAPPA). The eddy-permitting run is treated as a reference solution, and the differences between EDDY and COARSE results are considered what parameterization schemes should seek to achieve. EDDY has a horizontal resolution of  $1/8^\circ \times 1/8^\circ$ , and the coarse-grid and parameterized simulations have a horizontal resolution of  $2^\circ \times 1^\circ$ . The vertical resolution for all simulations is 39 levels with 10 m resolution for the top 200 m. Of course, even at  $1/8^\circ$  mesoscale eddies cannot be said to be properly resolved, and although still higher resolution could be achieved in a smaller domain, or for a single simulation over a short period, given the practical need for extended simulations in a domain that allows the eddy effects on the large-scale circulation to be gauged, these eddy simulations represent a reasonable attempt at a ground truth.

## 4. Results

### 4.1. Overturning circulation

For the residual run, since the momentum equation is now based on the residual velocity, the eddy velocity is calculated using (2.18) and the Eulerian velocity is calculated as the difference of the residual velocity and the eddy velocity. The mean overturning circulation streamfunction is defined as:

$$\Psi(y, z) = \int_z^\eta \int_{xw}^{xe} \bar{v} dx dz, \quad (4.1)$$

where  $\bar{v}$  is the Eulerian mean meridional velocity. The Eulerian mean overturning circulation is shown in Fig. 3 (from top to bottom: EDDY, COARSE, GMP\_1 and RS\_KAPPA\_1). A noticeable difference in mean overturning circulation for EDDY and COARSE is in the Deacon cell: the EDDY simulation has a very deep Eulerian meridional circulation in channel region. This is to be expected, because the channel region in our model is unblocked from top to bottom, thus there is no zonal pressure gradient or topography to maintain a lateral poleward velocity in the mid of ocean interior (see (2.8)); hence the downwelling in the low latitude end of the channel goes all the way down to the channel bottom. For COARSE, there is considerable lateral velocity in channel region, which arises because of a balance between the Coriolis force on the meridional flow and the horizontal viscosity,  $\nu_h \nabla^2 u$ . The latter term is needed to suppress noise and keep the model integrations stable; of course it is chosen to be as small as possible, but it is evident that it plays a non-negligible role in coarse resolution simulations, and there are

**Table 1**  
The configurations of experiments

Experiments	Residual scheme parameters			GM scheme parameters					
	$\nu_z$	$\nu_h$	$\kappa_z$	$\nu_e^{rs}$	$\nu_{max}$	$\kappa_{ml}$	$D_s$	$A_{gm}$	$S_{max}$
COARSE	$1 \times 10^{-4}$	$\sim 3.5 \times 10^4$	$2 \times 10^{-5}$	–	–	–	–	–	–
EDDY	$1 \times 10^{-4}$	$\sim 3.5 \times 10^4$	$2 \times 10^{-5}$	–	–	–	–	0.8	0.01
GMP_1	$1 \times 10^{-4}$	$\sim 3.5 \times 10^4$	$2 \times 10^{-5}$	–	–	–	–	1200	0.01
GMP_2	$1 \times 10^{-4}$	$\sim 3.5 \times 10^4$	$2 \times 10^{-5}$	–	–	–	–	1200	0.002
RS_KAPPA_1	$1 \times 10^{-4}$	$\sim 2.7 \times 10^4$	$2 \times 10^{-5}$	$1200f^2/N^2$	10	1200	100	–	–
RS_KAPPA_2	$1 \times 10^{-4}$	$\sim 2.7 \times 10^4$	$2 \times 10^{-5}$	$1200f^2/N^2$	2	1200	100	–	–
RS_KAPPA_3	$1 \times 10^{-4}$	$\sim 2.7 \times 10^4$	$2 \times 10^{-5}$	$1200f^2/N^2$	10	6000	100	–	–
RS_KAPPA_4	$1 \times 10^{-4}$	$\sim 2.7 \times 10^4$	$2 \times 10^{-5}$	$1200f^2/N^2$	10	12000	100	–	–
RS_KAPPA_5	$1 \times 10^{-4}$	$\sim 2.7 \times 10^4$	$2 \times 10^{-5}$	$1200f^2/N^2$	10	1200	0	–	–
RS_NU	$1 \times 10^{-4}$	$\sim 2.7 \times 10^4$	$2 \times 10^{-5}$	10	–	1200	100	–	–

See text for more details. EDDY uses a horizontal resolution of  $1/8^\circ \times 1/8^\circ$ , while the other experiments use  $2^\circ \times 1^\circ$ .  $\kappa_h = 0$  for all experiments. The EDDY experiment uses GM scheme but at a very low strength to reduce noise (not treated as eddy parameterization). Experiments RS\_KAPPA have a constant value of  $\kappa$ , with  $\nu_e^{rs} = \kappa f^2/N^2$ , and experiments RS\_NU have a constant value of  $\nu_e^{rs}$ . We ran all experiments for 50 years from the same initial condition which is resulted from a spin-up run (10,000-year run using COARSE configuration). The symbol “|” means the value is the same as that above.

significant differences in the zonally-averaged velocity fields between the eddying and coarse runs, especially the barotropic component. For COARSE and GMP,  $v_h \sim 3.5 \times 10^4 \text{ m}^2/\text{s}$ , and for residual run RS\_KAPPA, we find that we can use a somewhat smaller value,  $v_h \sim 2.7 \times 10^4 \text{ m}^2/\text{s}$ . Consistently, comparing to COARSE and GMP, residual run RS\_KAPPA\_1 does show some improvement in the Deacon cell. The fact that residual scheme can allow a lower horizontal viscosity seems to be because enhanced vertical friction term helps to remove noise; Ferreira and Marshall (2006), found an even larger effect.

Regarding the eddy overturning circulation (Fig. 4), in all three simulations (GMP\_1, RS\_NU, and RS\_KAPPA\_1), the direction of

eddy advection are mainly counter-clockwise (poleward in the top ocean and returning in ocean interior), and so largely cancels the mean overturning circulation (clockwise motion in channel). Compared to residual scheme experiments, the GM scheme seems to produce a noisier lower channel; this is because the eddy veloc-

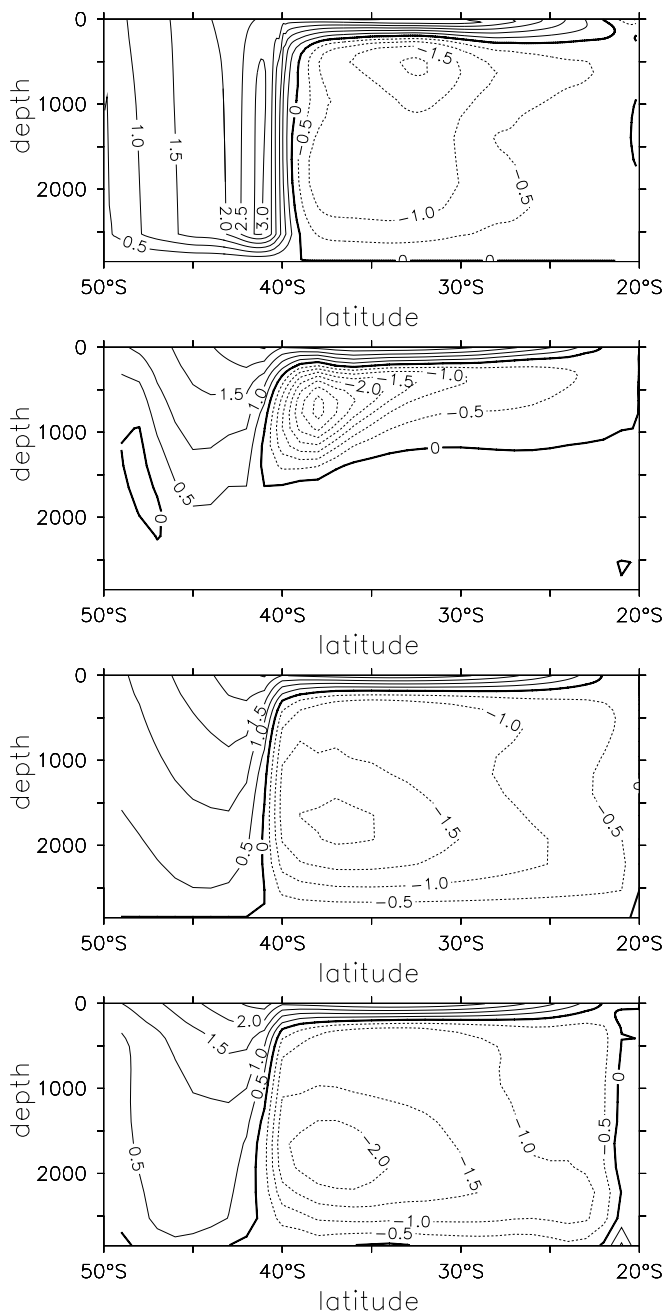


**Fig. 3.** Mean overturning circulation. From top to bottom: EDDY, COARSE, GMP\_1, and RS\_KAPPA\_1. Solid lines represent clockwise motion and dashed line anticlockwise motion. The streamlines are closed near the ocean boundaries (not shown). The meridional flow in the non-eddying runs in the channel is ageostrophic, and results from the horizontal friction term balancing the Coriolis term.

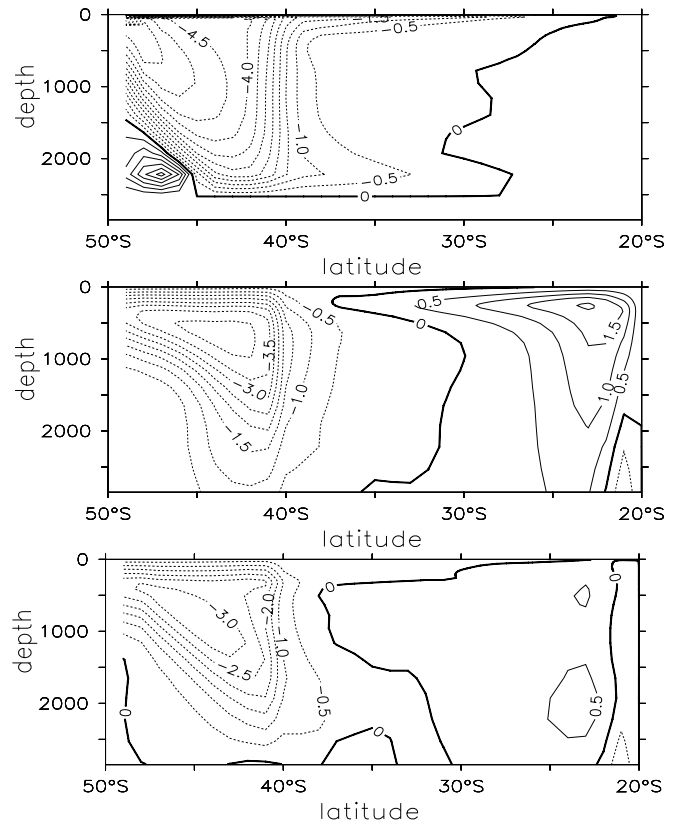


**Fig. 4.** Eddy overturning circulation ( $\Psi'(y,z) = \int_z^{\eta} \int_{xw} v' dx dz$ ), where  $v'$  is given by (2.24) for GM simulation and using (2.22) for residual simulations. From top to bottom: GMP\_1, RS\_NU, and RS\_KAPPA\_1. Solid lines represent clockwise motion and dashed line anticlockwise motion.

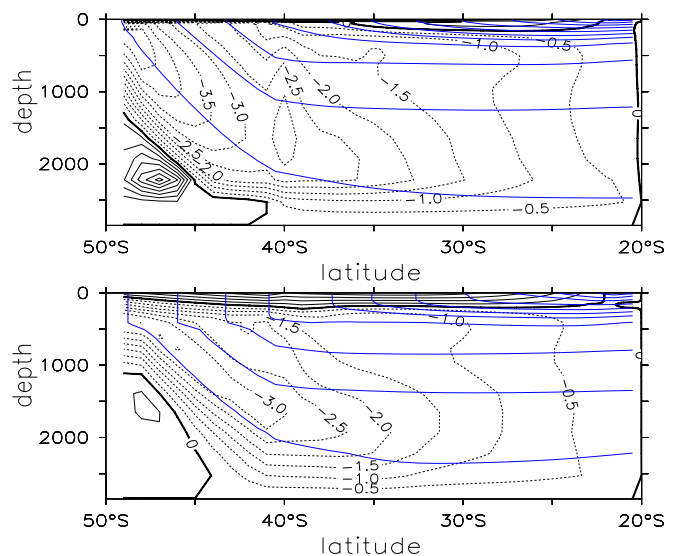


**Fig. 5.** Residual overturning circulation. Top: GMP\_1; bottom: RS\_KAPPA\_1. Solid lines represent clockwise motion and dashed line anticlockwise motion. The fainter solid lines show temperature, as in Fig. 6.

ity in GM parameterization relies on the vertical derivative of local isopycnal slope, and it tends to produce unphysical eddy flows in the region where it's very weakly stratified. The GM experiment also results in a much thinner mixed layer in the channel region, and more discussion about this will be found in Section 4.4. The residual simulation RS\_KAPPA\_1 (bottom panel) produces a rather cleaner eddy flux for the whole domain. It can also be shown in Fig. 5 (residual overturning circulation): for RS\_KAPPA\_1, residual flow follows isopycnals in ocean interior, and turns more horizontal in the top layer; while for GMP\_1, the flow is much more noisy.

We also ran a residual scheme simulation RS\_NU where  $v_e^{rs}$  is set to be a spatially constant. It was found the eddy circulation produced by RS\_NU (middle panel of Fig. 4) introduces eddy fluxes

in a highly stratified gyre region; these fluxes are not present in RS\_KAPPA simulations and seem to be unrealistically strong.

#### 4.2. Stratification and heat transport

Perhaps the most noticeable effect of the eddies is in the stratification. For a coarse-grid simulation that has no eddy parameterizations, unphysically weak stratification arises – note the almost vertical isopycnals in the channel region of COARSE (Fig. 6). The eddy-permitting simulation (EDDY) produces a realistic stratification – the isopycnals are largely slumped and available potential energy is released. Both GM parameterization and residual scheme simulations (two bottom panels of Fig. 6) are reasonably effective in this regard.

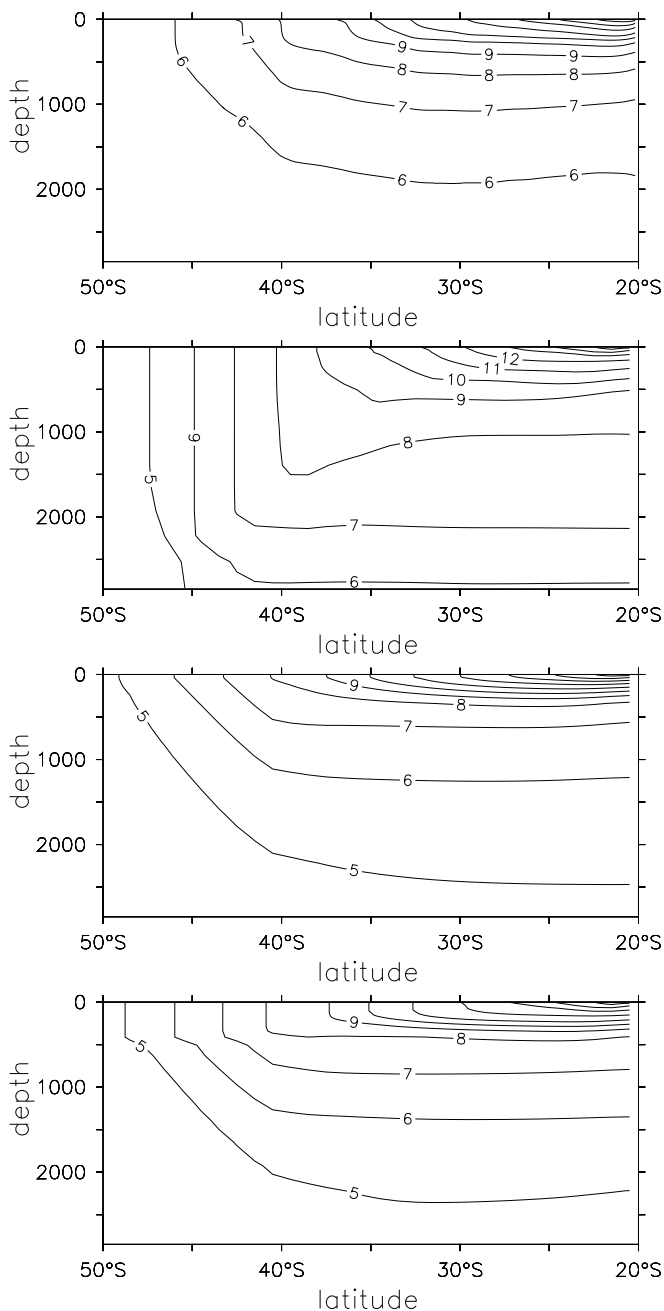


**Fig. 6.** Temperature contours. From top to bottom: EDDY; COARSE; GMP\_1, and RS\_KAPPA\_1. Both GM scheme and residual scheme are effective in slumping isopycnals in the channel region, thus the stratification resembles EDDY better.

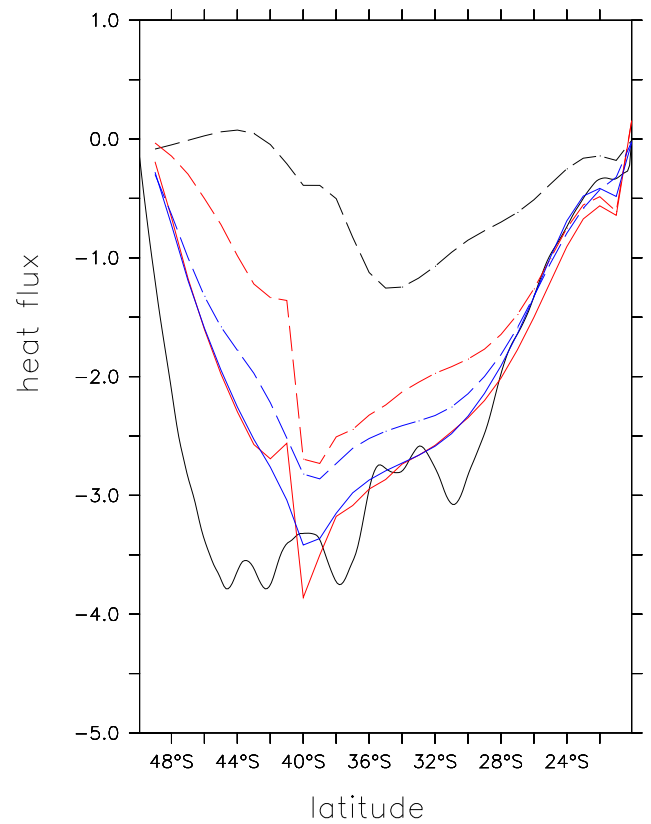


**Fig. 7.** Zonally and vertically-integrated meridional heat transport ( $10^{13}$  W). COARSE (---); EDDY (—); RS\_KAPPA\_1 (—); RS\_KAPPA\_2 (---); GMP\_1 (—); GM-P\_2 (---). Positive value means equatorward, negative value means poleward.

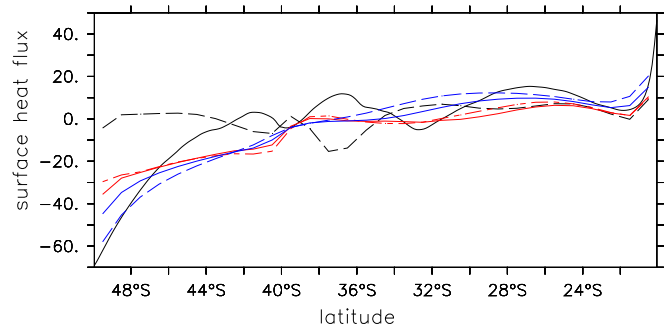


**Fig. 8.** Surface heat loss over the channel. EDDY (—); COARSE (---); GM\_1 (—); RS\_KAPPA\_1 (---); RS\_KAPPA\_3 (—); RS\_KAPPA\_4 (---). Negative value means heat loss.

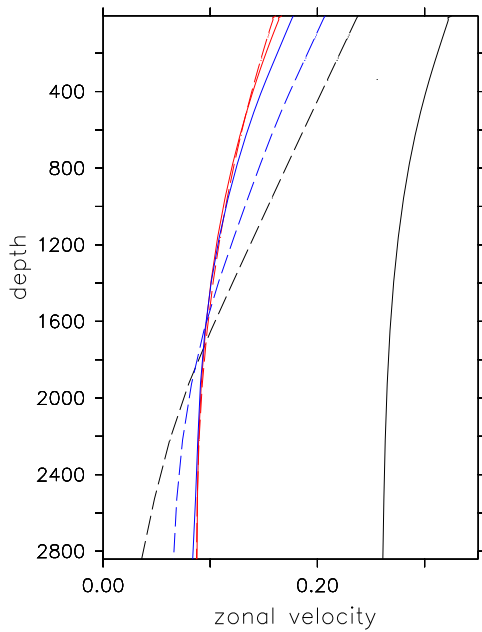


**Fig. 9.** Zonal velocity is averaged over entire channel both zonally and meridionally. COARSE (---); EDDY (—); RS\_KAPPA\_1 (—); RS\_KAPPA\_2 (---); GMP\_1 (—); GMP\_2 (---).

The total meridional heat transport,  $\rho C_p \int_z \int_x \overline{vT} dx dz$ , is plotted in Fig. 7, where negative value indicates that heat transport in the ocean is mainly poleward. The channel region is very active in the eddying simulation, full of mesoscale eddies that transport heat polewards. With no effective eddy parameterization scheme, COARSE has a cooler channel region than EDDY (Fig. 6) and weaker heat exchange between air and sea in the pole end (determined by the difference between SST and restoring temperature). Both GM and residual scheme simulation results show improvements for heat transport in channel region (data lines sit between EDDY

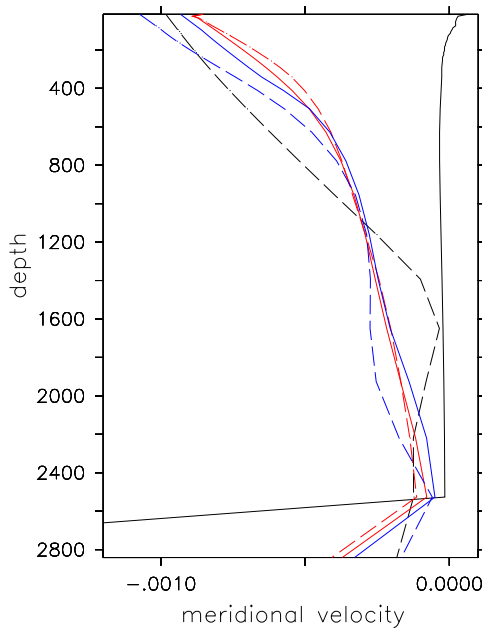


**Fig. 10.** Meridional velocity is averaged over entire channel both zonally and meridional, Ekman layer excluded. COARSE (---); EDDY (—); RS\_KAPPA\_1 (—); RS\_KAPPA\_2 (---); GMP\_1 (—); GMP\_2 (---).

and COARSE). The improvements in both schemes are done mainly by adding a poleward eddy velocity in the near surface region of the channel. Here we show two GM simulations, both with  $\kappa = 1200 \text{ m}^2 \text{ s}^{-1}$ , but with  $S_{\text{max}}$  of 0.002 to 0.01 respectively and two residual scheme simulations with  $v_{\text{max}} = 10$  or  $2 \text{ m}^2 \text{ s}^{-1}$ , respectively. (See Section 4.4 for the rationale of the choice of  $S_{\text{max}}$ . The larger value of  $S_{\text{max}}$  results in a larger poleward heat transport, because of a strong eddy circulation.) It indicates that the poleward heat transport is somewhat improved by increasing the value of  $v_{\text{max}}$  or  $S_{\text{max}}$ . Among the four parameterized simulations, the residual scheme with  $v_{\text{max}} = 10$  gives the closest simulation to EDDY.

As we noted previously, the diabatic process of lateral heat diffusion is not negligible in the top ocean surface diabatic layer, and in the GM scheme the tapering of the isopycnal mixing produces a horizontal, and so diabatic, mixing of buoyancy near the surface. We incorporate this effect in the residual scheme via the term  $\nabla_h \cdot (\kappa_{\text{ml}} \nabla_h T)$  in (3.8). This term plays a role in transporting heat down-gradient and has a direct influence on the surface heat exchange between the air and sea. We increase  $\kappa_{\text{ml}}$  (only applied to the top 100 m) from  $1200 \text{ m}^2/\text{s}$  (in RS\_KAPPA\_1 and RS\_KAPPA\_2) to  $6000 \text{ m}^2/\text{s}$  (RS\_KAPPA\_3) and then to  $12,000 \text{ m}^2/\text{s}$  (RS\_KAPPA\_4; Fig. 8). It is clear that higher eddy diffusivity helps to transport heat poleward, and the air-sea heat exchange at the pole end of the channel is largely enhanced: the surface heat loss at  $49^\circ\text{S}$  is almost doubled as  $\kappa_{\text{ml}}$  is increased from  $1200 \text{ m}^2/\text{s}$  to  $12,000 \text{ m}^2/\text{s}$ , with the latter solution better resembling the eddy-permitting results, although the comparison is still not perfect.

### 4.3. Zonal and meridional transport

Figs. 9 and 10 plot the zonal velocity and meridional velocity profiles against ocean depth. For zonal transports, the eddying run differs primarily in that it has a higher total zonal transport

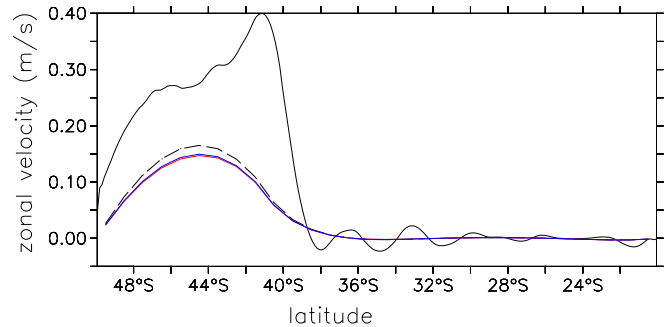


**Fig. 11.** Horizontal structure of zonal velocity (zonally and vertically averaged). EDDY (—); COARSE (---); RS\_KAPPA\_1 (—); GM\_1 (—).

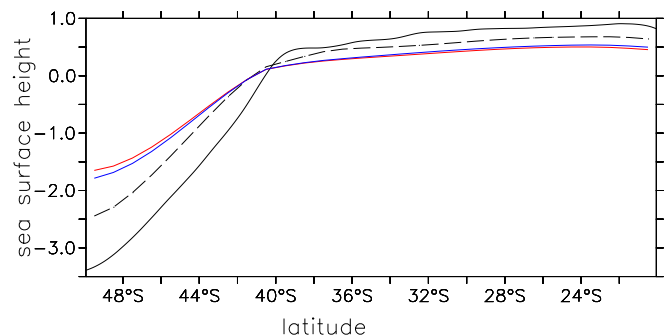


**Fig. 12.** Sea surface height. EDDY (—); COARSE (---); RS\_KAPPA\_1 (—); GM\_1 (—).

(vertically-integrated mass flux), primarily a barotropic transport. This partly a matter of friction: wall friction is only applied to the end grid box next to the wall, and for eddy-permitting run, this layer is much thinner comparing to coarse-grid simulations. Also, the eddying run results in a warmer and less stratified channel, hence  $P_y$  does not change much over depth therefore the vertical shear of  $u$  in eddying run is small too. The low transport is a feature of both the GM and residual runs, and is not a consequence of the larger vertical viscosity in the residual model. None of the eddy parameterization scheme shows improvement on zonal total transport over the scheme with high horizontal diffusion.

It seems that the eddy parameterization schemes (both the GM and residual scheme) improves vertical structure of zonal and meridional velocity (Fig. 9). A disadvantage for residual scheme is noted that both zonal and meridional velocity are now derived quantities from residual velocity and eddy velocity. But overall, we found both zonal and meridional velocity from residual scheme are close to the ones from GM scheme.

Although it is shown in Section 4.2 that eddy parameterization schemes help to improve the heat transport in the ocean, it is found that they do not have much influence on the vertically-inte-

grated mass transport. The solutions of vertically-integrated zonal transport and sea surface height are shown in Figs. 11 and 12, respectively. It is clear that the EDDY simulation results in a much higher zonal transport in the channel region, and also a much higher sea surface height gradient, but neither the residual scheme parameterization nor GM parameterization offers much improvement over the COARSE experiment. In some sense, their effects are actually working in an opposite way, that is, both GM and residual run result in a slightly lower zonal transport and SSH gradient than COARSE. (The positive side of the story is that the residual scheme and GM scheme give very similar results for the barotropic mode, despite significant differences in eddy parameterization implementations.) Certainly, the coarse models do not

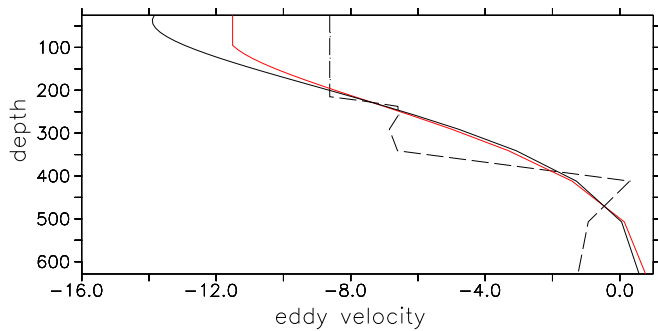


**Fig. 13.** Zonally integrated eddy velocity in channel center box (sv) for top 600 m. GM parameterization (---); residual scheme two-step tapering (—); and residual scheme one-step tapering (-·-). The GM parameterization tends to produce step-like changes in eddy velocity in the upper ocean, whereas the residual scheme is somewhat smoother.

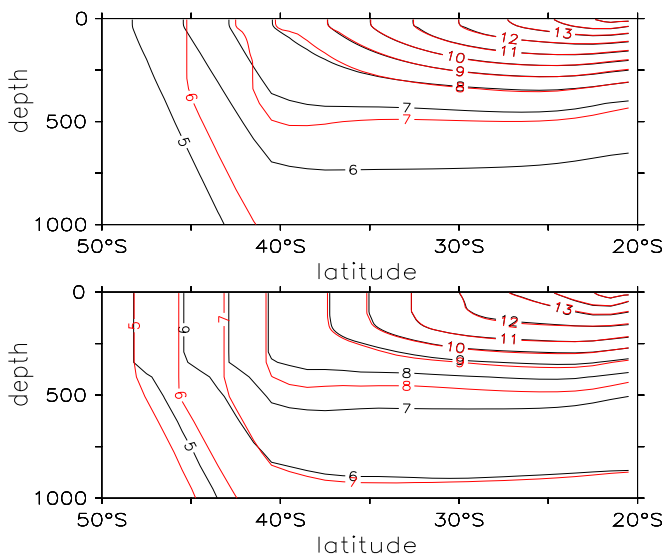


**Fig. 14.** Variation of  $S_{max}$  and  $v_{max}$  on stratification. Top: GMP\_1 (black) and GMP\_2 (red); Bottom: RS\_KAPPA\_1 (black) and RS\_KAPPA\_2 (red) (For interpretation of the references to colour in this figure legend, the reader is referred to the web version of this article.)

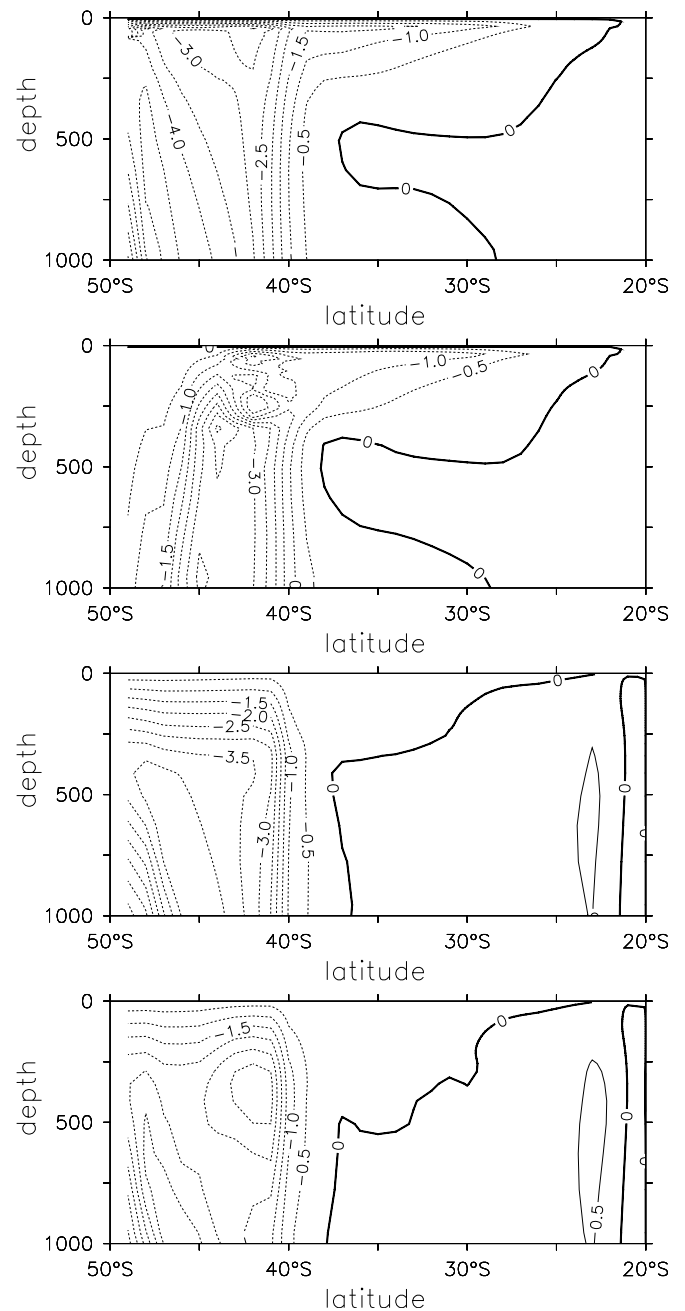


**Fig. 15.** Eddy overturning circulation for top 1000 m, obtained with two different values of  $S_{max}$  in the GM scheme (top two panels) and two different values of  $v_{max}$  in the residual scheme (bottom two panels). From top to bottom: GMP\_1; GMP\_2; RS\_KAPPA\_1; and RS\_KAPPA\_2.

account for any flux of momentum into the jet region by the eddies, and this may account for part of the difference.

#### 4.4. Variation of tapering parameters

As discussed in Section 2.3, one advantage of the tapering treatment of residual scheme is that it provides a gradual transition from ocean interior to the top diabatic layer. In contrast, slope tapering of the current GM parameterization in GFDL ocean model sometimes results in sharp shears in eddy velocity. Fig. 13 shows a comparison of the eddy velocity from both GM and residual simulations. The plotted lines in the figure are the eddy velocities at  $y = 45^\circ\text{S}$  (the center of the channel region) and zonally integrated. It is clear that for GM (dashed line), slope tapering results in a sharp shear in eddy velocity before it is tapered to be a constant for the top 300 m. For the residual scheme, the transition in  $v^*$  from ocean interior to top diabatic boundary layer happens in a much thicker layer (solid red line in Fig. 13), thus a very sharp shear in eddy velocity is avoided. It is noted that a smoother transition for  $v^*$  from ocean interior up not only improves numerical stability, but also it seems to avoid overly slumping local isopycnals, and thus is favored for both numerical and physical reasons. We might expect the residual scheme to give a relatively smooth transition from the ocean top to the interior, because the presence of a high viscosity and a relatively high Ekman number  $v_e/(fH^2)$  (compared to the integrations using GM) and large Ekman depth  $D_{\text{Ek}} = (v_e/f)^{1/2}$  will militate against jumps in the velocity field. A value of  $v_e = 10 \text{ m}^2 \text{ s}^{-1}$  (the maximum allowed value) gives  $D_{\text{Ek}} \approx 300 \text{ m}$ , although such a deep Ekman-like layer is not necessarily a realistic aspect of the residual scheme.

A set of simulations were performed to study the model sensitivity as we vary the tapering parameters. We ran two simulations with different tapering setting for both the residual scheme and GM. For GM,  $S_{\text{max}}$  is varying from 0.002 to 0.01. A corresponding

variation in  $v_{\text{max}}$  is approximately from 2 to 10 because, from (2.15),

$$\frac{v_e}{S} = \frac{\kappa f^2}{-(g/\rho_0)\rho_y} = \frac{\kappa f^2}{(g/\rho_0)\alpha T_y} \approx 10^3, \quad (4.2)$$

so that  $v_{\text{max}} \approx 10^3 S_{\text{max}}$ .

The top panel of Fig. 14 is used to show the model sensitivity on stratification to  $S_{\text{max}}$  in GM simulation. In the GM simulation the stratification for top channel becomes very different as  $S_{\text{max}}$  is changed from 0.002 to 0.01. In contrast, the stratification of residual scheme simulations is only slightly altered (bottom panel of Fig. 14) as  $v_{\text{max}}$  is changed from 2 to 10.

Fig. 15 shows a direct comparison between the eddy circulation streamfunction (top 1000 m) from both GM and RS\_KAPPA. The top two panels are GM simulations with  $S_{\text{max}}$  of 0.01 and 0.002, respectively. Evidently, the GM integrations give rather different diabatic surface layer as a different  $S_{\text{max}}$  is chosen:  $S_{\text{max}} = 0.01$  results in a very thin diabatic surface layer with high eddy velocity, whereas  $S_{\text{max}} = 0.002$  results in a thicker diabatic layer with low eddy velocity. The two bottom panels are residual simulations with  $v_{\text{max}}$  of 10 and 2, respectively. It is clear that the eddy flux in the residual simulation is much more stable to the variation of  $v_{\text{max}}$ .

We also tested a much more simple tapering treatment for residual scheme, that is, only  $v_e$  is capped using (2.20) and with no additional treatment to force eddy velocity to be constant for ocean top layer. A typical eddy velocity profile is shown in Fig. 13 (solid black line): there is a shear for eddy velocity throughout the surface boundary layer except the topmost boundary, where the eddy velocity has zero shear and wind forcing is purely applied to Eulerian mean velocity. This treatment is equivalent to the 2-step tapering of residual scheme but with  $D_s = 0$ . Compared this simple treatment to the residual 2-step treatment, we find that this simplification does not, in fact, make much difference on the model results except close to the surface. Fig. 16 shows both the

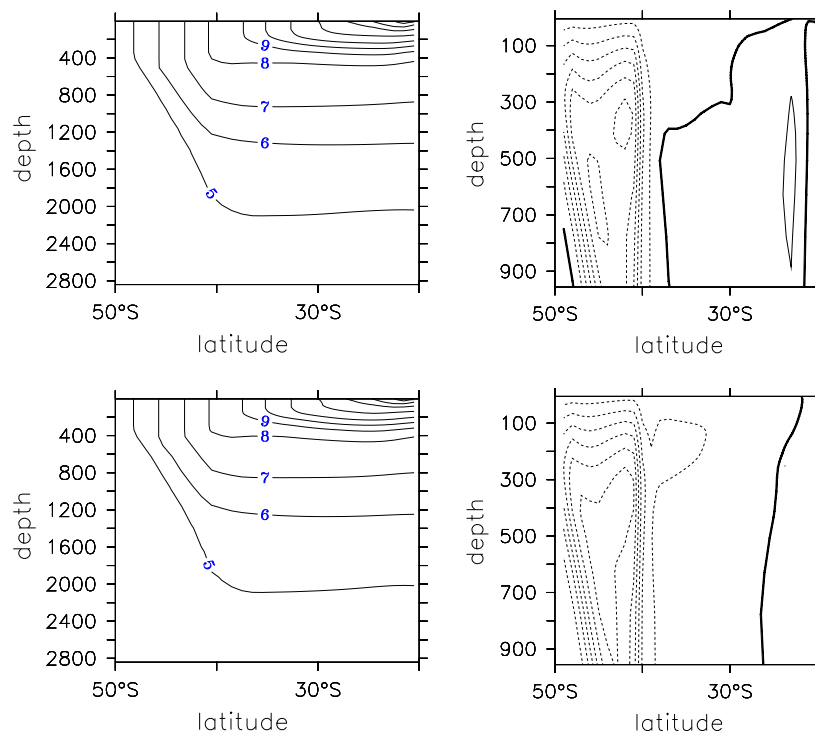


Fig. 16. Stratification(left) and eddy streamfunction(right). Upper panels (RS\_KAPPA\_5): eddy velocity is not enforced to be constant for the top surface diabatic layer in residual scheme; bottom panel (RS\_KAPPA\_1): eddy velocity is forced to be constant for the top 100 m.

stratification and eddy streamfunction (top 1000 m); both stratification and eddy circulation structure are in reasonably good agreement. This result is encouraging because it shows that the parameterization is not especially sensitive to rather ill-understood treatments of the mixed layer. The simple treatment also obviates the need to set  $D_s$ , which involves either an involved numerical calculation or an arbitrary guess, neither of which is wholly satisfying.

This improvement of residual scheme occurs mainly because its tapering treatment eliminates the abrupt change in eddy velocity that arises in the GM slope tapering treatment. It is possible that improvements may be realized by the use of a transitional layer beneath the mixed layer, but the exploration of that scheme is beyond the scope of this paper.

#### 4.5. Diffusing potential vorticity

Potential vorticity, being a materially conserved quantity, is in many ways a natural candidate for diffusion. (The first paper to discuss potential vorticity mixing in an ocean context was probably Welander (1973), followed by, and more explicitly looking at parameterizations, Marshall (1981), Treguier et al. (1997) and Greatbatch (1998). See Vallis (2006) for a general discussion of the matter.) However, in the implementations described above (both for the GM and residual schemes) we have not in fact included the gradient of potential vorticity due to planetary rotation; our schemes might be regarded as potential vorticity diffusion on the  $f$ -plane. In this section we redress that balance, and include the planetary vorticity gradient; however, at least in the simula-

tions that we have performed, we find that the effects are weak and the changes small.

For practical reasons we implemented potential vorticity mixing in the GM framework, by modifying the parameterized bolus velocity to be

$$\mathbf{v}_{pv}^* = \kappa \frac{\beta}{f} \mathbf{j} + \frac{\partial}{\partial z} \left( \frac{\nabla \bar{b}}{\partial_z \bar{b}} \right). \quad (4.3)$$

The conventional GM velocity is recovered if  $\beta = 0$ . In (4.3), the  $\beta$  term evidently induce a vertically integrated ('barotropic') flow that fails to satisfy the attendant kinematic constraints associated with potential vorticity fluxes; the effect is very small, at least in our simulations, and neglected. (In fact, over most regions of the world's oceans where eddying effects are important, the contribution of  $\beta$  to the potential vorticity gradient is small.)

We performed two simulations: one with a traditional GM scheme, and the other using (4.3). Both simulations are run 100 years from the same initial condition and other configurations. The results (Fig. 17) show that the additional  $\beta$  term makes little difference on the vertical structure of both temperature field and mass overturning. Diagnosis shows that the contribution the potential vorticity gradient in the model ocean from the  $\beta$  term is in fact quite small. With the additional  $\beta$  term, the model does show a small increase ( $\leq 10\%$ ) of sea surface heat flux in the high latitude region (bottom panel of Fig. 17), arising because of a slight increase in the eddy flux. Because the effect is small, we did not attempt to implement a fully self-consistent potential vorticity-based parameterization that satisfies the kinematic constraints (Treguier et al., 1997). Had we done so, we do not expect that significant changes would occur in these simulations, but we cannot discount the effects in other cases.

## 5. Conclusion

In this work, we have implemented and explored the effects of a residual scheme parameterization to account for mesoscale eddy effects on ocean general circulation. The scheme is formulated and implemented in GFDL Modular Ocean Model. The solutions are compared to those from eddy-permitting simulations, as well as coarse-grid simulations without eddy parameterizations apart from enhanced harmonic diffusivities and viscosities. The scheme is found to be generally effective in many aspects of the simulation of ocean general circulation. For example, it does flatten isopycnals and release potential energy to give a stratification that is much closer to that simulated in the eddying model. The residual scheme also produces an eddy circulation to effectively transport heat poleward so both heat transport and surface heat flux resemble the eddying run much better than does a coarse-grid simulation with only a diffusive parameterization. The scheme is also found to help improving zonal velocity structure in channel region.

We also explored the effects of diffusing potential vorticity by including a beta term in a GM-like parameterization. We found the effects to be generally small, and we speculate that many eddy rich regions of the ocean, in particular the ACC, the effects of including beta on a parameterization scheme will be small.

We implemented the residual scheme in two different general configurations: one uses a constant eddy viscosity  $\nu_e$  in the term  $\partial_z(\nu_e \partial_z u)$ ; the other uses constant eddy diffusivity  $\kappa$ , resulting in a vertically (and horizontally) varying  $\nu_e$ , which is a function of local  $N^2$ . Both are relatively easy to implement. In our simulations, we found that the scheme with constant  $\nu_e$  tends to give a larger eddy flux in highly stratified regions (such as gyre regions), and

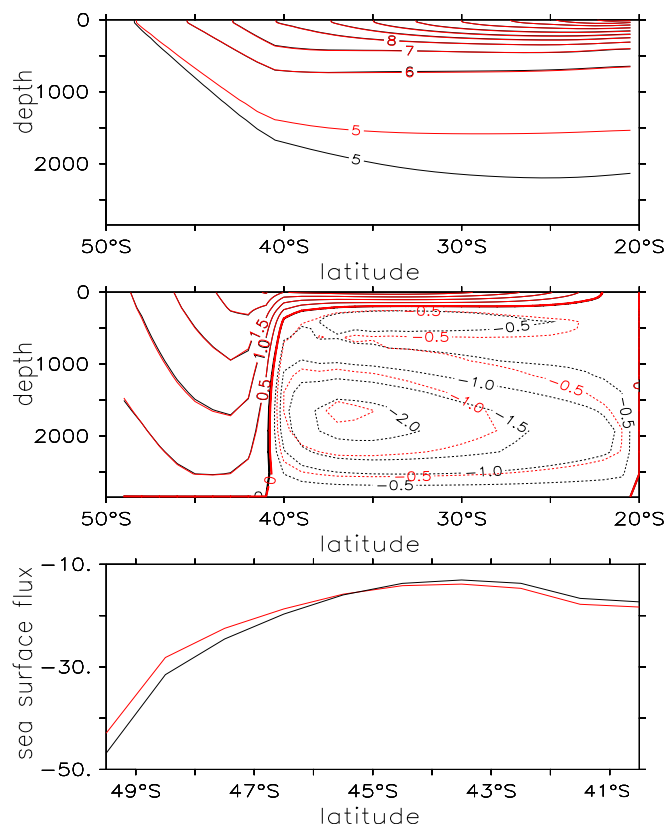


**Fig. 17.** A comparison between a traditional GM parameterization (red) and a revised scheme using eddy velocity defined in (4.3) (black): top: temperature contour ( $^{\circ}\text{C}$ ); middle: Eulerian overturning streamfunction (Sv); bottom: zonally integrated sea surface heat flux in the channel (MW/m).

results in a somewhat overly active eddy circulation there; this scheme generally compares less well with the eddy-permitting simulation. To improve the simulation in the gyre region, a horizontal structure could perhaps be applied to  $v_e$ , reducing its value at low latitudes (as in Ferreira and Marshall, 2006). However, the simpler residual scheme with constant  $\kappa$  (and so a variable  $v_e$  in the momentum equation, that is small in regions of high stratification) shows noted improvements over all other coarse-grid runs tested, and no geographical tuning of coefficients is needed. The addition of an enhanced horizontal buoyancy mixing in the upper ocean also provides improvement in the horizontal heat transport, emphasizing the important role of the surface diabatic layer.

The solutions are also compared to those from simulations that use a more traditional Gent-McWilliams (GM) parameterization. The residual scheme shows certain advantages in detail compared to GM. Primarily, the residual scheme seems less sensitive to the details of the implementation near the surface and to the details of the parameters. In this paper we explored various options, one in which we forced the eddy velocity to be constant over a mixed layer and another without such a constraint. In both cases we cap  $v_e$  to a maximum value where stratification is weak, in order to avoid numerical instability. Both cases achieve a gradual transition from ocean interior to the surface diabatic layer, and their model solutions agree with each other well except near the surface. In some contrast, we found GM to be rather sensitive to the tapering parameter  $S_{\max}$ , sometimes producing sudden shears in eddy velocity. Secondly, the residual scheme increases the numerical stability of coarse-grid runs by increasing vertical friction, enabling a rather lower horizontal friction to be used. The reduction is small in our simulations, but nonetheless welcome. Nonetheless, we certainly do not claim that the scheme is superior to the GM scheme.

The residual scheme has a somewhat simpler form than GM, and can be easily implemented by manipulating the vertical friction, with the caveat that, depending on the form of the implementation, isopycnal slopes must still be calculated. If there is more than one tracer in the model, the residual scheme only needs to be implemented in one equation (i.e., the momentum equation) rather than all the tracer equations, except that the Redi diffusion must still be calculated. The main disadvantage of the residual scheme for some purposes is that it uses residual velocity as the prognostic velocity, and so an additional computation may be needed to deduce Eulerian velocity.

Our overall conclusion is that the residual scheme is a viable alternative to the GM scheme. Compared to GM, the scheme is easier to implement in a model that has no salinity or passive tracers, and is comparably easy to implement in more realistic settings. The direct prediction of a residual velocity may be considered either an advantage or a disadvantage, depending on the setting and the desired use of the model. Neither GM nor the residual scheme are perfect, and both require tuning. Our feeling is that, ideally, an ocean model should provide both GM and a residual parameterization schemes, and the user may choose.

## Acknowledgement

We thank Richard Greatbatch and an anonymous reviewer for their useful comments. The work was funded by NSF and NOAA under a CPT on eddies and the mixed layer.

## Appendix A. Eddy streamfunction and eddy velocity

Expanding (2.4a,b), we have

$$\Psi = \frac{-1}{|\nabla \bar{b}|^2} \begin{vmatrix} \mathbf{i} & \mathbf{j} & \mathbf{k} \\ u'\bar{b}' & v'\bar{b}' & w'\bar{b}' \\ \bar{b}_x & \bar{b}_y & \bar{b}_z \end{vmatrix} \quad (\text{A.1})$$

and taking  $\bar{b}_x \ll \bar{b}_z$  and  $\bar{b}_y \ll \bar{b}_z$ ,  $\Psi$  can be simplified to give

$$\Psi \approx -\mathbf{i} \frac{v'\bar{b}'}{\bar{b}_z} + \mathbf{j} \frac{u'\bar{b}'}{\bar{b}_z} \quad (\text{A.2})$$

with a corresponding eddy velocity

$$\mathbf{v}^* = \begin{vmatrix} \mathbf{i} & \mathbf{j} & \mathbf{k} \\ \partial_x & \partial_y & \partial_z \\ -(v'\bar{b}')/\bar{b}_z & (u'\bar{b}')/\bar{b}_z & 0 \end{vmatrix} = \begin{bmatrix} -\partial_z(u'\bar{b}')/\bar{b}_z \\ -\partial_z(v'\bar{b}')/\bar{b}_z \\ \partial_x(u'\bar{b}')/\bar{b}_z + \partial_y(v'\bar{b}')/\bar{b}_z \end{bmatrix}. \quad (\text{A.3})$$

## References

- Andrews, D.G., Holton, J.R., Leovy, C.B., 1987. *Middle Atmosphere Dynamics*. Academic Press.
- Eden, C., Greatbatch, R.J., Olbers, D., 2007. Interpreting eddy fluxes. *J. Phys. Oceanogr.* 37, 1282–1296.
- Ferreira, D., Marshall, J., 2006. Formulation and implementation of a “residual-mean” ocean circulation model. *Ocean Modell.* 13, 86–107.
- Gent, P.R., McWilliams, J.C., 1990. Isopycnal mixing in ocean circulation models. *J. Phys. Oceanogr.* 20, 150–155.
- Gent, P.R., Willebrand, J., McDougall, T.J., McWilliams, J.C., 1995. Parameterizing eddy induced transports in ocean circulation models. *J. Phys. Oceanogr.* 25, 463–474.
- Gnanadesikan, A., Griffies, S.M., Samuels, B.L., 2007. Effects in a climate model of slope tapering in neutral physics schemes. *Ocean Modell.* 16, 1–16.
- Gough, W.A., Welch, W.J., 1994. Parameter space exploration of an ocean general circulation model using an isopycnal mixing parameterization. *J. Mar. Res.* 773–796.
- Greatbatch, R.J., 1998. Exploring the relationship between eddy-induced transport velocity, vertical momentum transfer and the isopycnal flux of potential vorticity. *J. Phys. Oceanogr.* 28, 422–432.
- Greatbatch, R.J., Lamb, K.G., 1990. On parameterizing vertical mixing of momentum in non-eddy-resolving ocean models. *J. Phys. Oceanogr.* 20, 1634–1637.
- Greatbatch, R.J., Li, G., 1990. Alongslope mean flow and an associated upslope bolus flux of tracer in a parameterization of mesoscale turbulence. *Deep Sea Res.* 47, 709–735.
- Griffies, S.M., 1998. The Gent-McWilliams skew-flux. *J. Phys. Oceanogr.* 28, 831–841.
- Griffies, S.M., Gnanadesikan, A., Pacanowski, R.C., Larichev, V.D., Dukowicz, J.K., Smith, R.D., 1998. Isoneutral diffusion in a z-coordinate model. *J. Phys. Oceanogr.* 28, 805–830.
- Holloway, G., 1997. Eddy transport of thickness and momentum in layer and level models. *J. Phys. Oceanogr.* 27, 1153–1157.
- Kuo, A., Plumb, R.A., Marshall, J., 2005. Transformed Eulerian mean theory. II: potential vorticity homogenization, and the equilibrium of a wind- and buoyancy-driven zonal flow. *J. Phys. Oceanogr.* 175–187.
- Ledwell, J.R., Watson, A.J., Law, C.S., 1998. Mixing of a tracer in the pycnocline. *J. Geophys. Res.* 103 (C10), 21499–21530.
- Marshall, J.C., 1981. On the parameterization of geostrophic eddies in the ocean. *J. Phys. Oceanogr.* 11, 257–271.
- Redi, M.H., 1982. Isopycnal mixing by coordinate rotation. *J. Phys. Oceanogr.* 12, 1154–1158.
- Toole, J.M., Schmitt, R.W., Polzin, K.L., 1994. Estimates of diapycnal mixing in the abyssal ocean. *Science*, 1120–1123.
- Treguier, A.M., Held, I.M., Larichev, V.D., 1997. On the parameterization of the quasigeostrophic eddies in primitive equation ocean models. *J. Phys. Oceanogr.* 27, 567–580.
- Vallis, G.K., 2006. *Atmospheric and Oceanic Fluid Dynamics*. Cambridge University Press. p. 745.
- Wardle, R., Marshall, J., 2000. Representation of eddies in a primitive equation model by a PV flux. *J. Phys. Oceanogr.* 30, 2481–2503.
- Welander, P., 1973. Lateral friction in the ocean as an effect of potential vorticity mixing. *Geophys. Fluid Dynam.* 5, 101–120.